Research article

Inhibition of sugar-binding activity of Galectins-8 by thiogalactoside (TDG) attenuates secondary brain damage and improves long-term prognosis following intracerebral hemorrhage

Jingjing Song, Hongying Bai, Si Chen, Yuanyuan Xing, Jiyu Lou [*]

Department of Neurology, the Second Affiliated Hospital of Zhengzhou University, Zhengzhou, 450014, China

ABSTRACT

Galectins-8 (Gal-8), the tandem repeat sequences of the galectin family, can influence the pathophysiologic processes in neurological disorders. However, its effect on intracerebral hemorrhage and related mechanisms remains nebulous. Using collagenase VII-S-induced ICH in the left striatum of mice, we investigated the effects of Gal-8 on cellular and molecular immune inflammatory responses in hemorrhagic brain and evaluated the severity of short- and long-term brain injury. Our results showed that activated microglia in the periphery of hematoma in mice with intracerebral hemorrhage expressed Gal-8, while Gal-8 could regulate the expression of cytokines, such as HMGB-1 ($P = 0.0032$), TNF-α ($P = 0.0158$), and IL-10 ($P = 0.0379$). Inhibition of the glucose-binding activity of Gal-8 by thiogalactoside (TDG) significantly reduced the volume of cerebral hematoma ($P = 0.0241$) and hydrocephalus ($P = 0.0112$) during the acute phase of cerebral hemorrhage and improved the long-term prognosis. TDG can reduce acute-phase brain tissue injury and improve the prognosis by inhibiting the activation of immune-inflammatory cells in the periphery of hematoma and reducing the release of pro-inflammatory factors.

1. Introduction

Intracerebral hemorrhage (ICH) is a neurological disorder with high morbidity and mortality, accounting for 15 % of all strokes [1], with an incidence of 12–15/100,000 person-years, often accompanied by severe neurological deficits and a poor prognosis [2]. For the therapeutic aspects of acute cerebral hemorrhage, although early surgical removal has the potential effect to reduce brain tissue damage by relieving local ischemia or removing toxic chemicals, Class I evidence from clinical trials failed to show the significantly improved prognosis [3]. Current therapies for ICH focus on hindering the expansion of the hemorrhage, reducing clot volume in intracerebral and parenchymal hematomas, and targeting perihematomal edema and inflammation [4].

There was a study evaluating the predictive marker in patients with internal carotid disease [5].

Galactose lectins (Galectins), a family of mammalian lectins structured as carbohydrate-containing ligand molecules, are considered as potential modulators of brain microglia polarization, immune surveillance, neuro-inflammation, and neuroprotection, and are key regulators of immune responses in the brain [6], associated with various physiological and pathological conditions. Galectin-8 (Gal-8), a member of the galectin family of tandem repeat sequences, influences pathophysiologic processes in multiple sclerosis,

* Corresponding author. Department of Neurology, the Second Affiliated Hospital of Zhengzhou University, No.2 Jingba Road, Jinshui District, Zhengzhou, 450014, China.
E-mail address: JYLoujiyu@163.com (J. Lou).

primary lateral sclerosis, and Alzheimer's disease by modulating microglia activity in these diseases [7–9]. Gal-8 is expressed in both tumors [10] and normal tissues [11], intracranially, predominantly in the hippocampus, choroid plexus, and cerebrospinal fluid and is localized in microglia [7,11,12]. Thiogalactoside (TDG) inhibits Gal-8 sugar-binding ability [13], which is thought to have anti-inflammatory effects.

Gal-8 localizes to microglia, and increased expression of Gal-8 in brain tissue of patients with multiple sclerosis in the active phase is accompanied by an increase in the number of activated microglia [12,14]. As a major component of the innate immune system, microglia are rapidly activated after ICH in response to acute brain injury [15,16]. Activated microglia play a dual role in the pathophysiology of ICH. They express and secrete inflammatory factors, reactive oxygen species and toxic molecules that cause further brain tissue damage, blood-brain barrier disruption, and brain edema [17–19]. On the other hand, they secrete anti-inflammatory factors that modulate and promote brain tissue repair and hematoma clearance [20]. Therefore, anti-inflammatory strategies targeting microglia may have a potential therapeutic effect on ICH and improve neurological outcomes post ICH. However, data on the role of Gal-8 in ICH remain limited.

In this study, we investigated the potential role of Gal-8 in ICH. We hypothesize that the elevated expression of Gal-8 in the brain after ICH promotes microglia activation, which in turn affects the pathophysiological process of cerebral hemorrhage and regulates neurological prognosis. In addition, we evaluated residual lesion volume, myelin loss, and brain atrophy on day 28 and neurological deficits on days 1, 3, 7, 14, 21, and 28 after cerebral hemorrhage.

2. Materials and methods

2.1. Study animals

SPF-grade male C57BL/6 mice (10–12 months old, weighing 25–30 g) were purchased from the Experimental Animal Center of Zhengzhou University and housed in an SPF-grade animal house at our hospital, temperature maintained at 26 °C Celsius, *ad libitum* diet and water, and artificial circadian rhythm. The experimental protocols were approved by the Ethics Committee and all operations were performed in accordance with the rules and regulations established by the Animal Ethics Committee. All efforts made are aimed at minimizing the suffering of the mice. Animal experiments were also performed according to the ARRIVE guidelines.

2.2. Intracerebral hemorrhage mouse model

The ICH model was established by injection of collagenase into the left striatum of mice [21]. The surgery was performed using 3 % isoflurane inhalation anesthesia. Mice were fixed to the mouse stereotaxic apparatus using an ear bar. The left caudate nucleus was injected with 0.075 U of type VII collagenase using stereotactic injection. The caudate nucleus was positioned 0.6 mm anterior to bregma and 2.0 mm to the left, with a depth of 3.2 mm. Neurological function evaluation was performed by applying the modified neurological deficit score (NDS) 24 h following ICH model establishment [22]. In the experiment, NDS scores below 10 or above 18 on the first day post ICH were excluded. Mice with unsuccessful modeling were euthanized using intraperitoneal injection of an overdose of 0.3 % sodium pentobarbital.

2.3. Treatment regimens and experimental groups

The expression of Gal-8 at the site of cerebral hematoma and its effects on immune cell activation and infiltration, brain injury severity, and long-term neurological function following ICH was investigated.

The mice were randomly assigned into the following four groups with computer-generated random numbers: vehicle treated sham group, TDG treated sham group, vehicle treated ICH group and TDG treated ICH group. TDG powder was dissolved in ddH$_2$O and diluted to a solution of 1 mg/ml and injected intraperitoneally at a dose of 5 mg/kg 2 h post-surgery, every other day [13,23]. Mice were treated with the same volume of salt injection vector in 5 % DMSO.

2.4. Tissue processing, the volume of brain lesion, swelling, and atrophy

On day 1 and day 28 post ICH, mice were anesthetized with 0.3 % sodium pentobarbital (30 mg/kg) followed by transcardial perfusion with PBS and 4 % paraformaldehyde (PFA). Brain tissues were collected and placed in 4 % paraformaldehyde solution in 4 °C refrigerator overnight. Brain tissues were then transferred to 20 % sucrose solution for 24 h and 30 % sucrose solution for 48 h. The brain tissue completely sank to the bottom of the tube lumen, embedding with an embedding agent. Brain tissue was divided into one 50 μm section and twelve 30 μm sections from the level of the olfactory bulb to the visual cortex for a total of 10 cycles using a frozen sectioning machine. Brain tissue sections (50 μm) were stained with Luxol fastblue (LFB) for myelin and Cresyl Violet (CV) for nerves to measure brain injury volume, white matter damage, brain swelling, and atrophy, meanwhile 30 μm brain tissue sections were stored in antifreeze solution and used for immunofluorescence staining and FJB staining.

Brain injury volumes were measured on day 1 or day 28 following ICH using Image Analyisis software on LFB/CV stained 50 μm sections ($n = 10$/group for day 1 and n = 4/group for day 28). The area of brain tissue not stained with LFB/CV is the site of brain injury. The specific formula is as follows: brain hemorrhage volume/residual lesion volume = sum of hemorrhage area at each level × slice thickness [24].

Brain swelling was measured on the first day following ICH ($n = 10$/group). Volumes were measured in the ipsilateral and

contralateral hemispheres using Image Analyisis software. The degree of brain swelling was calculated as: (volume of the cerebral hemisphere on the hemorrhagic side – volume of the contralateral cerebral hemisphere)/volume on the hemorrhagic side $\times$ 100 % [25, 26].

The degree of brain atrophy was calculated on day 28 after ICH ($n = 10$/group), which was consistent with the measurement of the degree of brain swelling. The degree of cerebral atrophy was calculated as: (volume of the contralateral cerebral hemisphere – volume of the hemorrhagic side of the cerebral hemisphere)/volume of the hemorrhagic side $\times$ 100 % [24,26].

2.5. Brain water content

The mice in each group were successfully modeled and anesthetized with 0.3 % pentobarbital sodium intraperitoneally at 24 h. The mice were euthanized via cervical dislocation, and the brain tissue was divided into the ipsilateral cerebral hemisphere, the contralateral cerebral hemisphere, and the cerebellum and weighed immediately with an electronic molecular balance, which was the wet weight (WW). The tissues were then baked in a 100 °C oven for at least 24 h until the weight remained constant and weigh again to obtain the dry weight (DW). The brain tissue water content was then calculated according to the Eliot formula: brain water content (BWC)＝(WW – DW)/WW $\times$ 100 % [24,27].

2.6. Evaluation of neurological deficits

Neurological function was assessed in mice on day 1, 3, 7, 14, 21, and 28 ($n = 12$/group) using a modified NDS score and a corner test. The NDS score was divided into 6 items, namely body symmetry, gait, climbing test, spontaneous turning behavior, mandatory turning, and forelimb symmetry. Each test was scored on a scale of 0–4, with 0 being no neurological deficit and 4 representing the most severe neurological deficit.

The corner test is an asymmetric behavioral test used to evaluate rodents after ICH [28]. Mice typically exhibit good turning defects within 24 h of injury, turning asymmetry has not fully recovered, and this persists for up to 4 weeks. The mice were placed in a 30 °C corner and rotated to the left or right by placing one or both front paws on the wall as they moved their bodies from side to side. Fifteen consecutive trials were performed at 30s intervals. The percentage of left turns for each mouse was used as the corner test score.

2.7. Immunofluorescence double staining of paraffin sections

Brain tissue was placed in a 4 % PFA solution for 24 h, rinsed with tap water for 24 h, and sequentially subjected to gradient dehydration and clearing, wax dipping, embedding, and making paraffin sections. Paraffin sections of each brain tissue were selected at a similar level, deparaffinized to water, and placed in 1 $\times$ citric acid antigen repair solution for antigen repair. Then, 5 % BSA 50 μl was added dropwise into the water-blocking ring and closed for 30 min at room temperature. Next, 30 μl Gal-8 antibody (1:50, AB69631, Abcam) was added dropwise on the slide and incubated overnight at 4 °C in the refrigerator protected from light. On the following day, 50 μl of the corresponding 488 (1:1,000, 016-540-084, Jackson) was added dropwise to the water-blocking ring after gently shaking the slide and incubated for 60 min at room temperature in the dark. Using the same steps, the tissue was also incubated with Iba-1 antibody (1:1000; 019–19741, Dako) and cy3 antibody (1:1,000, Jackson). Finally, 4′,6-Diamidino-2-phenylindole dihydrochloride (DAPI) staining solution was added dropwise and incubated for 3–5 min at room temperature away from light, followed by neutral dendrimer sealing.

2.8. Frozen section immunofluorescence

Four brain slices of similar dimensions were selected for each brain tissue specimen and immunofluorescence staining was performed ($n = 6$/group). The steps were as follows: brain tissue sections were rinsed in 1 $\times$ PBS buffer, 0.1 % phosphate Tween (PBST) buffer, and 0.3 % PBST buffer 3 times, 5 min each time. Brain slices were blocked in 5 % donkey serum solution and incubated at room temperature for 1 h, and incubated with primary antibody overnight at 4 °C. The primary antibodies used were rabbit anti-glial fibrillary acid protein (GFAP, Astrocyte marker, 1:200; 16825-1-AP, Proteintech), rabbit anti-ionized calcium-binding adapter molecule 1 (Iba-1, microglial/macrophage maker, 1:1000; 019–19741, Dako), rabbit anti-myeloperoxidase (MPO, neutrophil maker, 1:150; ab9535, Abcam). Tissues were rinsed 3 times with 0.3 % PBST buffer solution for 5 min each time, then incubated with secondary antibody (anti-rabbit Cy3,1:1000, Jackson; anti-rabbit 488, 1:1,000, 016-540-084, Jackson) for 1 h at room temperature in the dark. After the final rinse with 0.3 % PBST buffer solution 3 times, the nuclei were stained with 1–2 drops of 5 % DAPI staining solution and observed under the microscope and photographed (Zeiss, AXIO OBSERVER 3).

2.9. Fluoro-Jade B staining (FJB)

FJB staining was used to detect degenerative neurons around the hematoma 24 h post ICH ($n = 6$/group). Three brain slices of similar level were selected for each mouse, FJB staining and photographic observation under a fluorescent microscope (wave-length 450–490 nm) were used to quantify the degenerating neurons in the same manner as the measurement of immune-inflammatory cells.

2.10. Western blotting

The hemorrhagic lateral brain tissue was rapidly separated and placed in liquid nitrogen ($n = 4$/group). The brain tissue on the hemorrhagic side was lysed by the cell lysate (20 μl of protease inhibitor, 10 μl of phosphatase inhibitor A, 10 μl of phosphatase inhibitor B, and 10 μl of phenylmethanesulfonyl fluoride (PMSF) per 1 ml of RIPA lysate) and total protein was extracted. Protein concentration was determined using the BCA method. The protein samples were heated at 100 °C for 10 min. The same amount of protein was transferred to PVDF membranes following electrophoresis, separation gels of 10 % and 12 % were prepared according to the molecular weight of the tested proteins. PVDF membranes were blocked with 5 % skim milk for 1 h at room temperature and incubated overnight at 4 °C with primary mouse antibodies against TNF-α (1:1,000, 60291 Proteintech), IL-10 (1:1,000, 60269, Proteintech) and rabbit antibodies, HMGB-1 (1:1000; 10829, Proteintech) and TGF-β1 (1:3,000, 21898, Proteintech). On the following
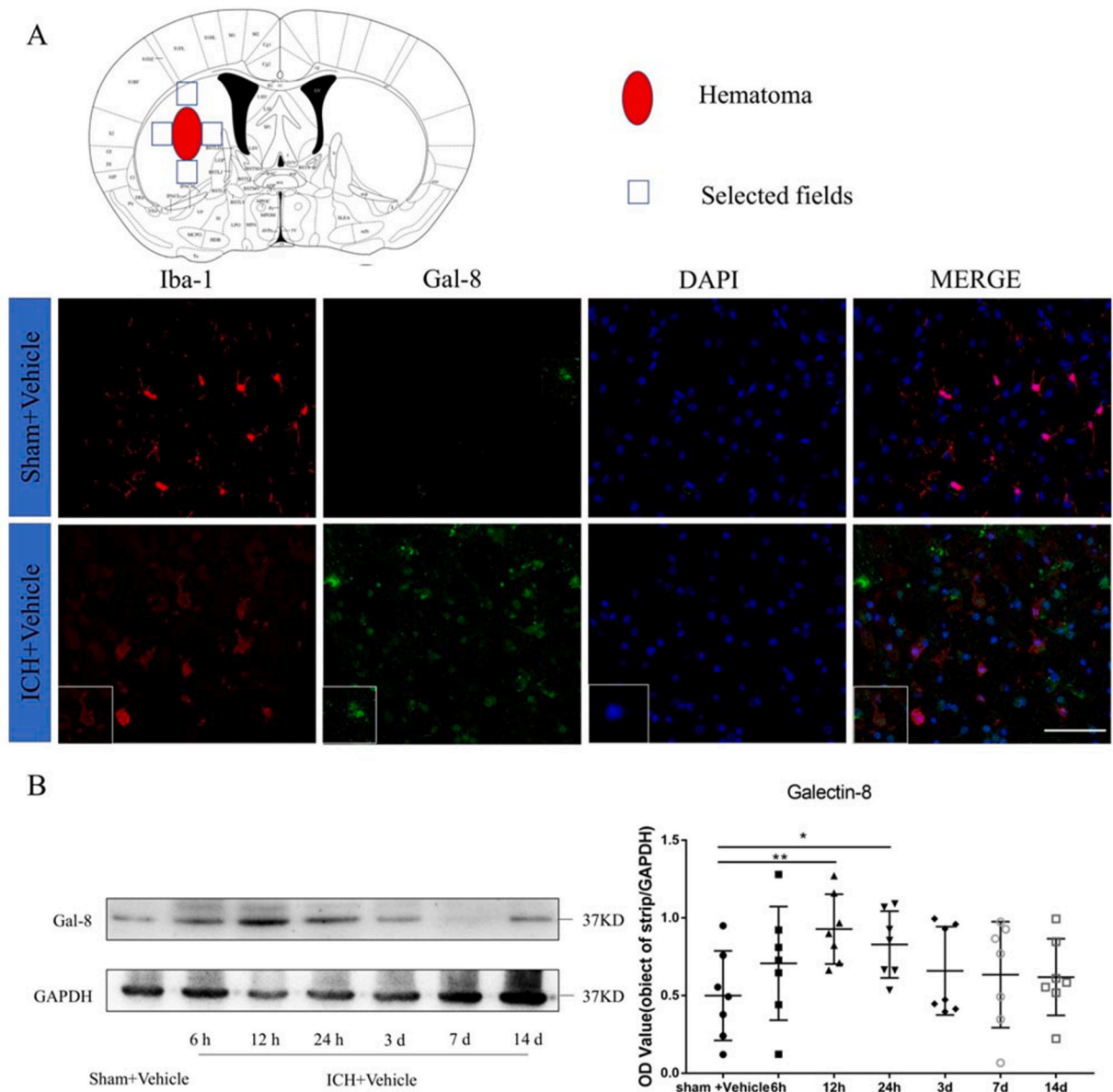
Fig. 1. Increased expression of Gal-8 within 24 h of ICH. A, Localization of Gal-8 expression in microglia surrounding hematoma in mice with cerebral hemorrhage. Iba-1 (red), Gal-8 (green) ($n = 5$/group, Scale bar = 50*um*). B, Representative Western blot of Gal-8 at different time points post ICH; GAPDH was used as the loading control. Scattergrams showing the quantitative analysis of Gal-8 expression at different time points following ICH. Densitometric quantification suggested that the increased expression of Gal-8 appeared 6 h after ICH, peaked at 12 h ($P = 0.0058$), and lasted until 24 h ($P = 0.0424$); $n = 5$/group. (For interpretation of the references to colour in this figure legend, the reader is referred to the Web version of this article.)
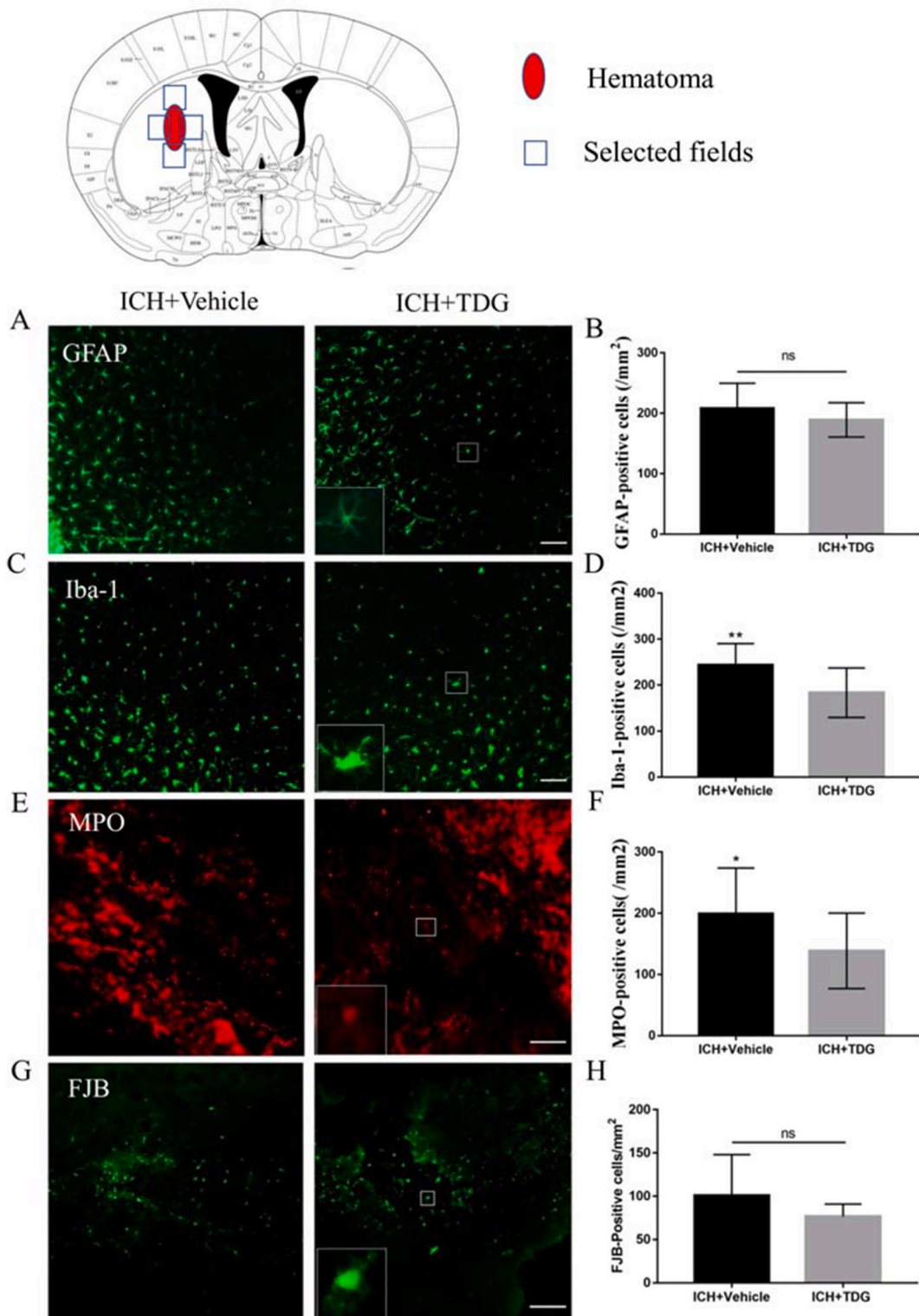
Fig. 2. TDG treatment reduced neutrophil infiltration and microglia activation but had no significant effect on the number of FJB-positive cells and astrocytic activation on day 1 post ICH. (A, C, E, G) Representative images of immunofluorescence staining for Iba-1 (C), GFAP (A), and MPO (E) in the perihematomal region on day 1. Scale bar = 100um. (B, D, F, H) Bar graphs showing the quantitative analysis of Iba-1- (F), GFAP- (G), MPO- (H), and FJB- (I) positive cells. n = 6/group. Iba1, ionized calcium-binding adapter molecule 1; GFAP, glial fibrillary acid protein; MPO, myeloperoxidase; FJB, Fluoro-Jade B.

day, the membranes were incubated with secondary antibodies (HRP-labeled goat anti-rabbit, 1:3000; 511203, ZEN BIO, HRP-labeled goat anti-mouse, 1:3000; 511103, ZEN BIO) for 2 h at room temperature, and rinsed with Tris-Buffered Saline with Tween 20 (TBST). ECL ultrasensitive luminescent solution was used for (BMU102-CU, SuperKine ™) exposure development.

2.11. White matter damage and myelin loss

White matter damage was quantified using 30 μm sections on day 28 post ICH ($n = 12$/group), which were stained in advance with LFB. Three different stained sections and four sites per section were selected in each mouse and photographed under a light microscope at the same exposure level to visualize myelin. Image J software was used to count the sum of the white matter areas in each region, divide it by the total area of the image, and obtain the percentage of white matter.

2.12. Statistical analysis

GraphPad Prism 9.5.1 and SPSS 26.0 software was used to analyze and plot all experimental data. Data were presented as mean ± standard error (mean ± SEM). Comparisons between groups were analyzed using Student's *t*-test or one-way ANOVA for normally distributed continuous variables. When ANOVA showed significant differences, post hoc Bonferroni test was used for pairwise comparisons. Between-group comparisons of repeated measures over time was performed using two-way ANOVA (two-way ANOVA). Statistical significance was set at $P < 0.05$.

3. Results

3.1. Gal-8 expression increased around the hematoma and localized to activated microglia following ICH

The brain tissues were paraffin embedded after 4 % PFA fixation and selected Iba-1 as a microglia surface marker (red) and Gal-8 (green) for immunofluorescence double staining, and the nuclei were stained with DAPI (blue). The morphology of microglia in the brain tissue of mice in the vehicle-treated sham-operated was highly branched, while the morphology of microglia around the hematoma in the vehicle-treated ICH group of mice changed from a branching shape to an amoeboid shape with increased cell volume and shorter or absent protrusions, which is the activated morphology of microglia. There was no Gal-8 expression around the hematoma in the vehicle-treated sham-operated group mice, and Gal-8 expression was significantly increased in the peripheral region of the hematoma in the vehicle-treated ICH group mice and co-localized with activated microglia (Fig. 1A).

Brain tissue proteins were taken from ICH model mice and the protein expression of Gal-8 at the hematoma site at different time
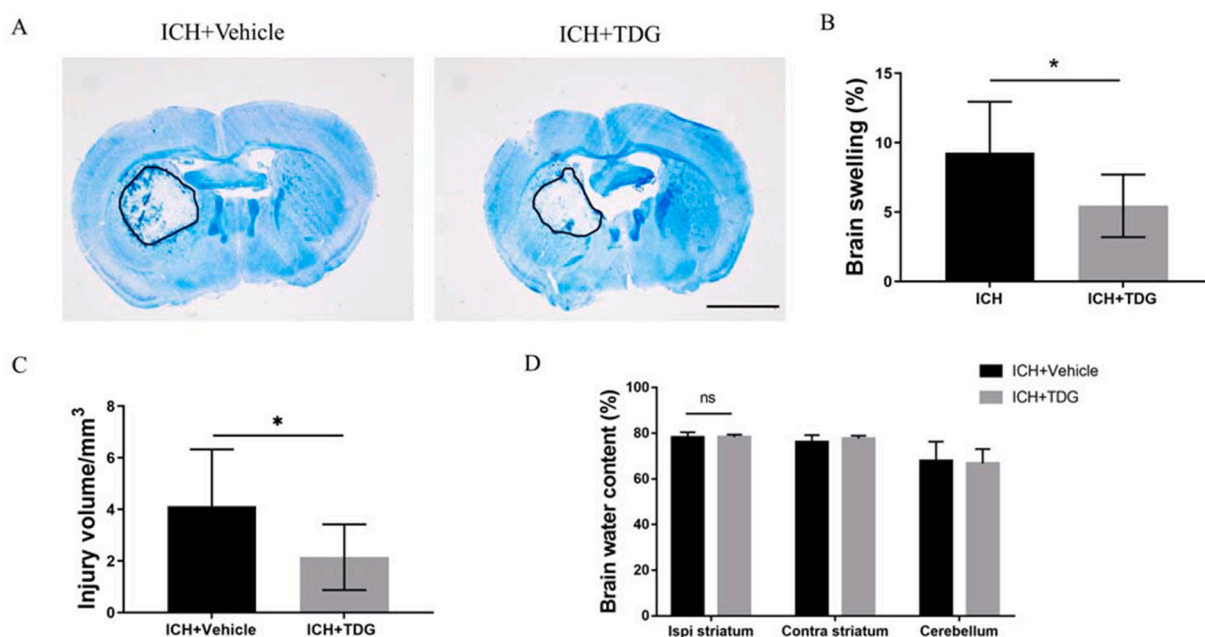
Fig. 3. TDG treatment decreased brain swelling on day 1 post ICH. (A) Representative brain sections stained with LFB/CV on day 1 post ICH. Black curves circle areas of lesions lacking staining. Scale bar = 1 mm. (B) On day 1 post ICH, TDG treatment did not decrease the water content of the ipsilateral striatum. $n = 6$/group. (C) Brain damage volume was measured in LFB/CV-stained brain sections. TDG treatment did not reduce brain injury volume compared with the vehicle-treated group on day 1 post ICH. $n = 6$/group. (D) TDG treatment decreased brain swelling on day 1 post ICH. $n = 6$/group. Data are expressed as mean ± SD. Ipsi, ipsilateral; Contra, contralateral.

points (6, 12, and 24 h, and days 3, 7, and 14) was detected using Western blot. The increased expression of Gal-8 appeared at 6 h post ICH, peaked at 12 h ($P = 0.0058$), and lasted until 24 h ($P = 0.0424$), as shown in Fig. 1B and C ($n = 5$/group). Protein expression at the remaining time points was also elevated compared with the vehicle treated sham-operated group, although the differences were not statistically significant.

TDG inhibited neutrophil infiltration and microglia activation but had no significant effect on the activation of degenerating neurons and astrocytes.

GFAP was selected as a surface marker for astrocytes and Iba-1 as a surface marker for microglia. Based on the morphological characteristics of activated microglia, the number of activated microglia around the hematoma was significantly lower in the TDG treated ICH group compared with the vehicle treated ICH group treated on day 1 after ICH ($n = 6$/group, $P= 0.0244$, Fig. 2C and D). However, based on the strong immune-reactivity of GFAP and the morphological characteristics of reactive astrocytes, there was no significant difference in the number of astrocytes between the TDG treated ICH group and the vehicle treated ICH group ($n = 6$/group, $P = 0.2728$, Fig. 2A and B).

MPO was chosen as the surface marker of neutrophils and found that the number of neutrophils around the hematoma was significantly lower in the ICH group treated with TDG compared with mice in the ICH group treated with vehicle on 1 day after ICH ($n = 6$/group, $P = 0.0230$, Fig. 2E and F).

Brain tissue sections was subjected to FJB staining to visualize the degenerated neurons around the hematoma following ICH. It was found that mice in the TDG treated ICH group did not have a significantly lower number of degenerated neurons compared with those in the vehicle treated ICH group ($n = 6$/group, $P = 0.1892$, Fig. 2G and H).

3.2. TDG treatment decreased brain swelling and brain lesion volume but did not affect edema post ICH

LFB/CV staining was performed on day 1 following ICH to determine the effect of Gal-8 on brain injury volume and swelling. The missing, unstained part of the brain tissue is the area of brain damage (Fig. 3A). Brain swelling measured as a percentage of hemispheric enlargement, it showed that on day 1 after ICH, TDG treatment significantly reduced brain swelling compared to the vehicle treated ICH group (Fig. 3B, $n = 10$/group, $P = 0.0135$). Further analysis also indicated that the TDG treatment also significantly reduced the volume of brain damage compared to the vehicle treated ICH group (Fig. 3C, $n = 10$/group, $P = 0.2423$). However, neither ICH nor TDG influenced the water content in the ipsilateral striatum, contralateral striatum and cerebellum on day 1 after surgery (Fig. 3D, $n = 5$/group P values for the ipsilateral striatum, contralateral striatum and cerebellum were 0.133 and 0.065, respectively).
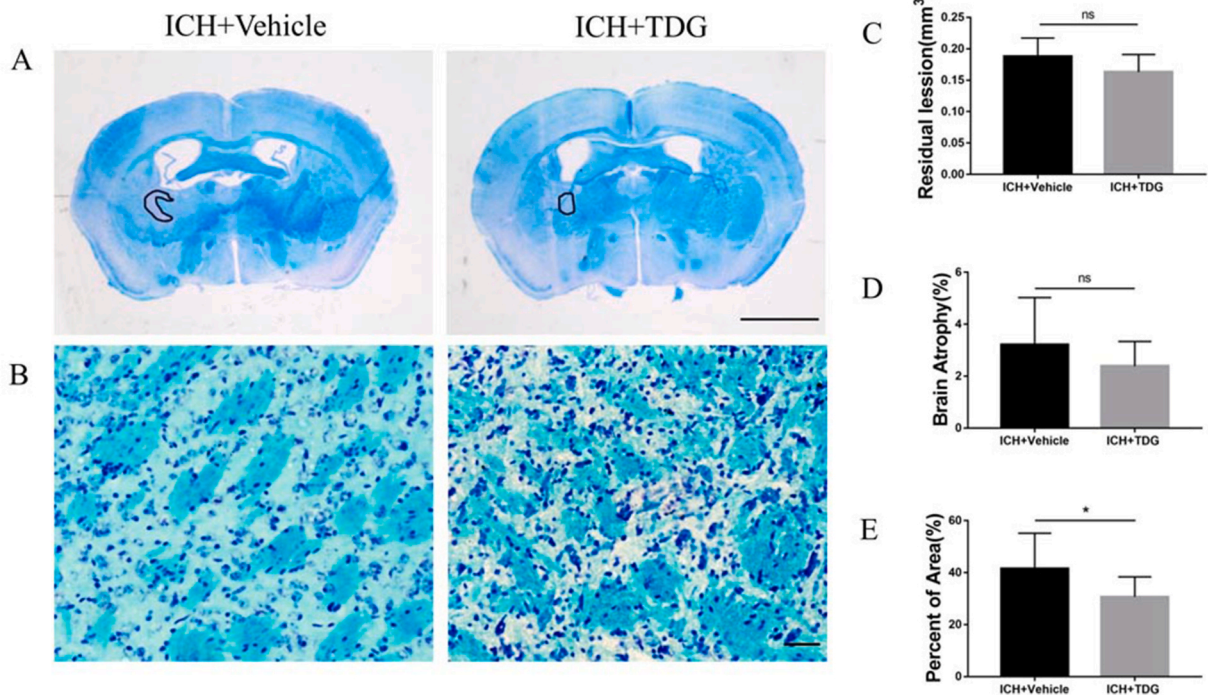
Fig. 4. TDG attenuated cerebral white matter damage at day 28 post ICH. (A) Representative images of brain sections stained with LFB/CV on day 28. The areas of the lesions are indicated in circled with the black curve; scale bar = 1 mm. (B) LFB-stained myelin from brain sections in the perihematomal region on day 28. Scale bar = 1 mm. (C, D) Brain damage volume and degree of atrophy were measured in LFB/CV-stained brain sections. Bar graphs show the quantitative analysis of residual lesion volume (C) and brain atrophy (D). (E) Quantitative analysis of white matter damage. Treatment with TDG reduced the loss of LFB-stained myelin in the perihematomal region. $n = 10$/group.
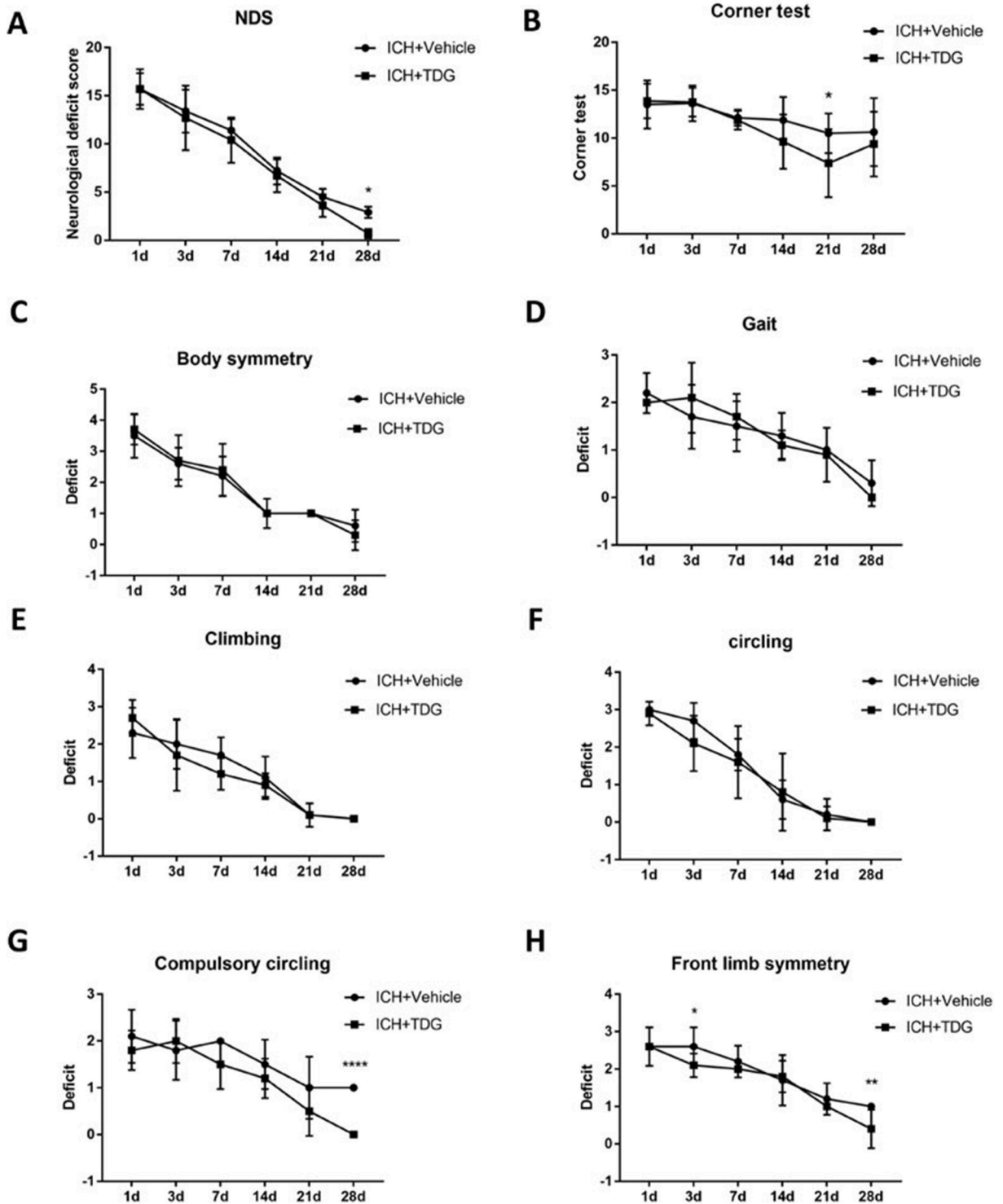
Fig. 5. TDG treatment improved long-term neurologic deficits after ICH. (A) Compared with the ICH group treated with vehicle, TDG treatment improved neurologic function evaluated with neurological deficit scores (NDS) in mice on day 28. (B) Treatment with TDG reduced the rate of left-turning on day 21 of cerebral hemorrhage. (C–H) Neurological deficit scores for individual tests on days 1, 3, 7, 14, 21, and 28. $n = 10$/group. *$P < 0.05$, **$P < 0.01$, ****$P < 0.0001$.

TDG treatment significantly reduced white matter damage, but had no significant effect on residual lesion volume or brain atrophy on day 28 after ICH.

The volume of residual lesions, brain atrophy, and white matter damage on day 28 following ICH were measured (Fig. 4A and B). Brain tissue sections from mice treated with TDG or vehicle on day 28 following ICH were selected for LFB/CV staining. TDG significantly reduced white matter damage around the peri-residual lesions compared to the vehicle treated ICH group ($n = 10$/group, $P = 0.0444$) on day 28 following ICH. However, no significant effect on residual lesions and brain atrophy was observed ($P = 0.3028$ for residual lesions, $P = 0.4470$ for brain atrophy, $n = 4$/group) (Fig. 4C, D, E).

3.3. TDG treatment improved the long-term neurologic function of ICH

The NDS scores of mice in the vehicle or TDG treated ICH group were the highest on day 1 post ICH and gradually decreased. While the TDG treatment had lower NDS than the vehicle treated ICH group on day 28 post ICH ($P = 0.0374$ on day 28, $n = 10$/group, Fig. 5A). The test results for the individual scoring indicators are as follows (Fig. 5). Front limb symmetry on days 3, 28, and compulsory circling on day 28 were significantly lower in the TDG treated ICH group compared with those of the vehicle-treated group following ICH ($P = 0.0129$ for front limb symmetry on day 3, $P = 0.0018$ for front limb symmetry on day 28, $P < 0.0001$ for compulsory circling on day 28, $n = 10$/group, Fig. 5G and H). The corner turn test score is quantified by the left turn rate. TDG treatment
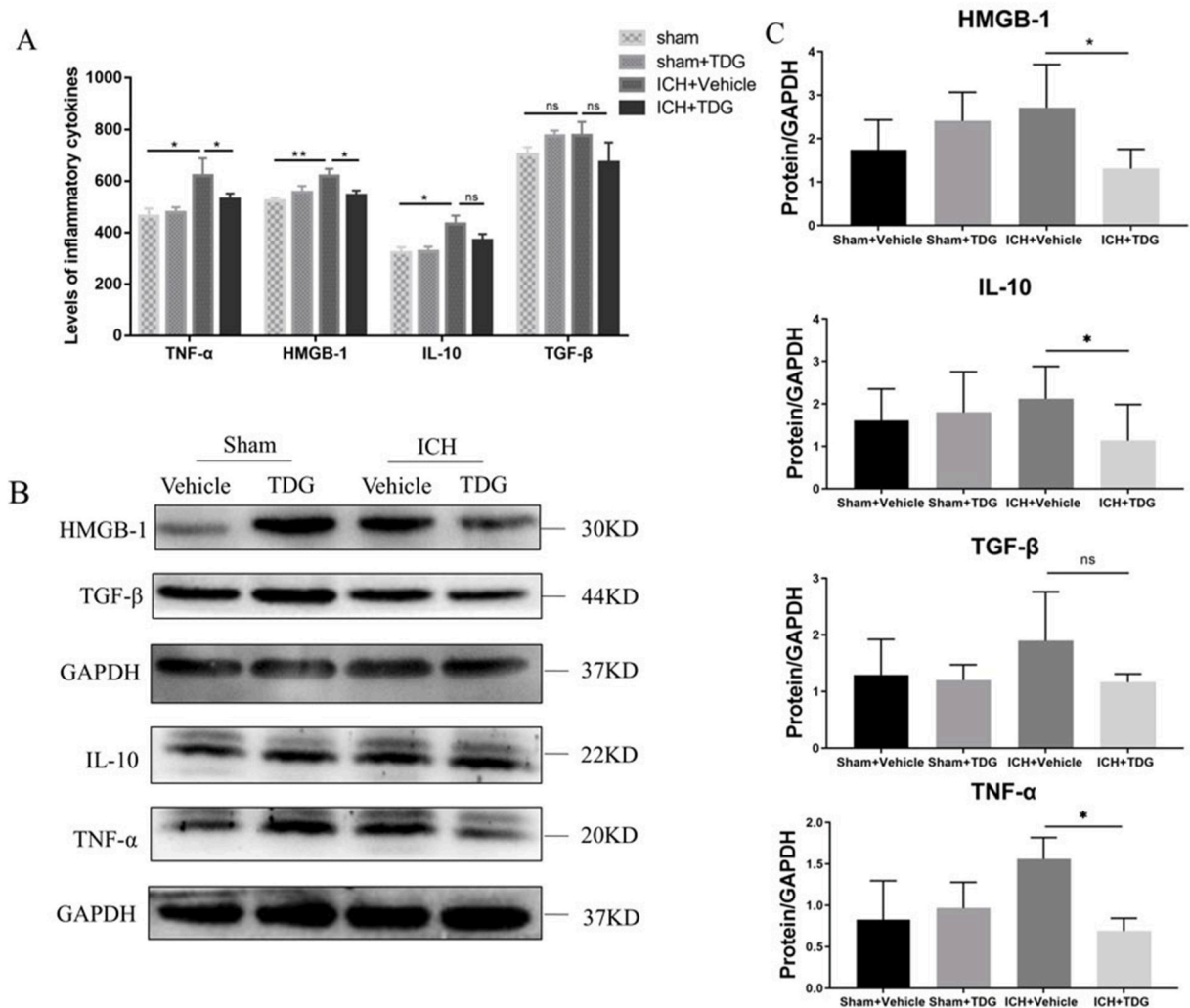
Fig. 6. Gal-8 promoted cytokine production. (A) ELISA kits were used to detect relative concentration levels of inflammatory factors HMGB-1, TNF-α, IL-10, and TGF-β in peripheral blood. TDG treatment reduced peripheral blood concentrations of HMGB-1 and TNF-α. $n = 5$/group. (B) Representative Western blot bands of proinflammatory factor HMGB-1, TNF-α, IL-10, and TGF-β; GAPDH was used as the loading control. (C) Bar graphs showing the expression of HMGB-1, TNF-α, IL-10, and TGF-β at 24 h post ICH. Densitometric quantification suggested that TDG treatment significantly decreased the levels of HMGB-1, TNF-α, and IL-10 levels and reduced TGF-β levels; however, it did not reach statistical significance. *$P < 0.05$.

significantly reduced the rate of left turn in mice on day 21 post ICH ($P = 0.0443$, $n = 10$/group, Fig. 5B). There were no significant differences of body symmetry, galt, climbing and circling between TDG treated ICH group and vehicle-treated ICH group. ($P > 0.05$, $n = 10$/group, Fig. 5C–F).

3.4. TDG reduced the expression of pro-inflammatory factors

The levels of inflammatory factors in peripheral serum were significantly higher after ICH compared with the sham-operated group ($n = 5$/group, $P = 0.0054$ for HMGB-1, $P = 0.0005$ for TNF-α, $P = 0.028$ for IL-10) (Fig. 6A and B). Mice in the ICH group treated with TDG possessed lower levels of HMGB-1 and TNF-α in peripheral serum compared with those in the vehicle treated ICH group ($n = 5$/group, $P = 0.0313$ for HMGB-1, $P = 0.0387$ for TNF-α). However, there was no significant difference in the concentration levels of IL-10 and TGF-β in peripheral blood serum between the mice in the ICH group treated with vehicle or TDG ($n = 5$/group, $P = 0.2991$ for IL-10, $P = 0.0517$ for TGF-β) (Fig. 6A and B).

The measurement in brain tissue were similar to those of the expression of inflammatory factors in peripheral serum. TDG treatment significantly reduced the expression of HMGB-1, TNF-α, and IL-10 at the hematoma site compared with the vehicle treated ICH group ($n = 5$/group, TNF-α: $P = 0.0065$, HMGB-1: $P = 0.0238$, IL-10: $P = 0.0468$). However, IL-10 expression was not statistically significant, although it decreased to some extent (Fig. 6C).

4. Discussion

It was found that Gal-8 is expressed in brain tissue, and is involved in acquired and innate immune responses in the central nervous system [29]. However, data on how Gal-8 functions against cerebral hemorrhagic disease remain limited. Based on histomorphometric observations, we found that TDG inhibited the sugar-binding activity of Gal-8 and significantly reduced the volume of cerebral hematoma and the degree of brain swelling. It suggests that Gal-8 exerts neurotoxic effects after cerebral hemorrhage and aggravates secondary brain damage of cerebral hemorrhage to some extent.

A study of brain tissue from multiple sclerosis patients in active and remission reported that Gal-8 expression was increased in brain tissue in the active phase compared with the chronic phase and was positively correlated with the number of activated microglia [14]. From this, we can speculate that Gal-8 expression and microglia activation are closely linked. Microglia, as resident cells within the central nervous system and play an important role in the immune inflammatory response after cerebral hemorrhage. Microglia activated after brain hemorrhage evokes innate immune responses and promotes the production of inflammatory mediators when danger signals are perceived [30,31]. Microglia activation can drive neuro-inflammation, oxidative stress, and cytotoxic cascade responses leading to cell death and dysfunction [32]. Gal-8 is secreted and expressed by vascular endothelial cells and platelets [14,33, 34]. It have been showed that Gal-8 was mainly localized in microglia [12]. The number of activated microglia in the peripheral region of the hematoma revealed that the number of activated microglia in the peripheral region of the hematoma decreased following the inhibition of the sugar-binding activity of Gal-8, thus confirming, even more, that Gal-8 promotes the activation of microglia [12].

Interactions between microglia and astrocytes and neutrophils jointly regulate the immune inflammatory response following cerebral hemorrhage [35]. *In vitro* and *in vivo* assays have shown that microglia activation releases IL-1α, TNF-α, and complement component subunit 1q (C1q) to induce A1-type reactive astrocyte production [36,37]. In addition, microglia activation after cerebral hemorrhage can secrete chemokines such as CXCL1 and CCL2 to chemotactic neutrophils and monocytes to migrate into the brain [38], aggravating secondary brain injury post cerebral hemorrhage.

It has also been found that the CRD at the Gal-8 C terminus binds to integrin Am/CD11b and proMMP-9 to regulate neutrophil function [39]. Our results revealed that inhibition of the sugar-binding activity of Gal-8 by TDG significantly reduced the number of neutrophils in the periphery of the hematoma, while the number of astrocytes was not significantly altered. This suggests that Gal-8 promotes neutrophil infiltration into the hematoma periphery to some extent through microglia activation, aggravating secondary brain injury.

Gal-8 increased the secretion of chemokines and cytokines (i.e., IL-2, MCP-5, IL-6, MCP-1, TNF-α, and IL-3) from bone marrow-derived dendritic cells [40] and is a potent inducer of functional disease markers such as IL-1B, TNF-α, IL-6, MMP-1, MMP-3, and MMP-13 [41]. Based on these findings, we investigated the expression of inflammatory factors in the periphery of hematoma post ICH and found that the inhibition of sugar-binding activity by TDG significantly reduced the expression levels of the inflammatory factors HMGB-1 and TNF-α. The experimental results suggest that Gal-8 is involved in regulating the immune-inflammatory response after cerebral hemorrhage by promoting cytokine expression. However, the exact mechanism remains to be determined. The signaling pathway Gal-8 involved in regulating immune inflammation post ICH still needs to be followed up with further studies.

In conclusion, this study showed that inhibition of the sugar-binding activity of Gal-8 attenuated secondary brain injury post ICH, which in turn demonstrated the neurotoxic effect of Gal-8 on secondary injury. Gal-8 has a significant therapeutic potential for ICH and is a potential target for intervention in the treatment of cerebral hemorrhage.

Data availability statement

Data will be made available on request.

Ethics declarations

Funding

CRediT authorship contribution statement

Jingjing Song: Writing – original draft, Resources, Methodology, Investigation, Formal analysis, Conceptualization. **Hongying Bai:** Writing – review & editing, Resources, Methodology, Investigation, Data curation. **Si Chen:** Writing – review & editing, Validation, Software, Resources, Methodology, Investigation. **Yuanyuan Xing:** Writing – review & editing, Visualization, Validation, Methodology, Investigation, Data curation. **Jiyu Lou:** Writing – review & editing, Supervision, Resources, Project administration.

Declaration of competing interest

The authors declare that they have no known competing financial interests or personal relationships that could have appeared to influence the work reported in this paper.

Acknowledgements

Appendix A. Supplementary data

Supplementary data to this article can be found online at https://doi.org/10.1016/j.heliyon.2024.e30422.

References

[1] A.I. Qureshi, S. Tuhrim, J.P. Broderick, H.H. Batjer, H. Hondo, D.F. Hanley, Spontaneous intracerebral hemorrhage, N. Engl. J. Med. 344 (2001) 1450–1460.
[2] M.T. Poon, A.F. Fonville, Salman R. Al-Shahi, Long-term prognosis after intracerebral haemorrhage: systematic review and meta-analysis, J. Neurol. Neurosurg. Psychiatry 85 (2014) 660–667.
[3] D.G. Nehls, D.A. Mendelow, D.I. Graham, G.M. Teasdale, Experimental intracerebral hemorrhage: early removal of a spontaneous mass lesion improves late outcome, Neurosurgery 27 (1990) 674–682. ; discussion 682.
[4] M.N. Al-Kawaz, D.F. Hanley, W. Ziai, Advances in therapeutic approaches for spontaneous intracerebral hemorrhage, Neurotherapeutics 17 (2020) 1757–1767.
[5] S. Aslan, A.R. Demir, Y. Demir, Ö. Taşbulak, M. Altunova, M. Karakayalı, E. Yılmaz, İ. Gürbak, M. Ertürk, Usefulness of plateletcrit in the prediction of major adverse cardiac and cerebrovascular events in patients with carotid artery stenosis, Vascular 27 (2019) 479–486.
[6] F. Barake, A. Soza, A. González, Galectins in the brain: advances in neuroinflammation, neuroprotection and therapeutic opportunities, Curr. Opin. Neurol. 33 (2020) 381–390.
[7] E. Pardo, C. Cárcamo, R. Uribe-San Martín, E. Ciampi, F. Segovia-Miranda, C. Curkovic-Peña, F. Montecino, C. Holmes, J.E. Tichauer, E. Acuña, F. Osorio-Barrios, M. Castro, P. Cortes, C. Oyanadel, D.M. Valenzuela, R. Pacheco, R. Naves, A. Soza, A. González, Galectin-8 as an immunosuppressor in experimental autoimmune encephalomyelitis and a target of human early prognostic antibodies in multiple sclerosis, PLoS One 12 (2017) e0177472.
[8] J.F. Sampson, A. Suryawanshi, W.S. Chen, G.A. Rabinovich, N. Panjwani, Galectin-8 promotes regulatory T-cell differentiation by modulating IL-2 and TGFβ signaling, Immunol. Cell Biol. 94 (2016) 213–219.
[9] L. Massardo, C. Metz, E. Pardo, V. Mezzano, M. Babul, E. Jarpa, A.M. Guzmán, S. André, H. Kaltner, H.J. Gabius, A. Jacobelli, A. González, A. Soza, Autoantibodies against galectin-8: their specificity, association with lymphopenia in systemic lupus erythematosus and detection in rheumatoid arthritis and acute inflammation, Lupus 18 (2009) 539–546.
[10] N. Bidon-Wagner, J.P. Le Pennec, Human galectin-8 isoforms and cancer, Glycoconj. J. 19 (2002) 557–563.
[11] Y.R. Hadari, K. Paz, R. Dekel, T. Mestrovic, D. Accili, Y. Zick, Galectin-8. A new rat lectin, related to galectin-4, J. Biol. Chem. 270 (1995) 3447–3453.
[12] J.J. Siew, Y. Chern, Microglial lectins in health and neurological diseases, Front. Mol. Neurosci. 11 (2018) 158.
[13] W.S. Chen, Z. Cao, S. Sugaya, M.J. Lopez, V.G. Sendra, N. Laver, H. Leffler, U.J. Nilsson, J. Fu, J. Song, L. Xia, P. Hamrah, N. Panjwani, Pathological lymphangiogenesis is modulated by galectin-8-dependent crosstalk between podoplanin and integrin-associated VEGFR-3, Nat. Commun. 7 (2016) 11302.
[14] M. Stancic, J. van Horssen, V.L. Thijssen, H.J. Gabius, P. van der Valk, D. Hoekstra, W. Baron, Increased expression of distinct galectins in multiple sclerosis lesions, Neuropathol. Appl. Neurobiol. 37 (2011) 654–671.
[15] J. Gehrmann, Y. Matsumoto, G.W. Kreutzberg, Microglia: intrinsic immuneffector cell of the brain, Brain Res Brain Res Rev 20 (1995) 269–287.
[16] Z. Yang, T. Zhao, Y. Zou, J.H. Zhang, H. Feng, Curcumin inhibits microglia inflammation and confers neuroprotection in intracerebral hemorrhage, Immunol. Lett. 160 (2014) 89–95.
[17] Y.N. Jassam, S. Izzy, M. Whalen, D.B. McGavern, J. El Khoury, Neuroimmunology of traumatic brain injury: time for a paradigm shift, Neuron 95 (2017) 1246–1265.
[18] X. Lan, X. Han, Q. Li, Q.W. Yang, J. Wang, Modulators of microglial activation and polarization after intracerebral haemorrhage, Nat. Rev. Neurol. 13 (2017) 420–433.

[19] Z. Zhang, Z. Zhang, H. Lu, Q. Yang, H. Wu, J. Wang, Microglial polarization and inflammatory mediators after intracerebral hemorrhage, Mol. Neurobiol. 54 (2017) 1874–1886.

[20] J. Liu, L. Liu, X. Wang, R. Jiang, Q. Bai, G. Wang, Microglia: a double-edged sword in intracerebral hemorrhage from basic mechanisms to clinical research, Front. Immunol. 12 (2021) 675660.

[21] L.C. Huang, H.K. Liew, H.Y. Cheng, H.F. Peng, H.I. Yang, J.S. Kuo, W.L. Hsu, C.Y. Pang, Collagenase-induced rat intra-striatal hemorrhage mimicking severe human intra-striatal hemorrhage, Chin. J. Physiol. 60 (2017) 259–266.

[22] W.M. Clark, N.S. Lessov, M.P. Dixon, F. Eckenstein, Monofilament intraluminal middle cerebral artery occlusion in the mouse, Neurol. Res. 19 (1997) 641–648.

[23] V.V. Prabhu, J.E. Allen, D.T. Dicker, W.S. El-Deiry, Small-molecule ONC201/TIC10 targets chemotherapy-resistant colorectal cancer stem-like cells in an akt/foxo3a/TRAIL-dependent manner, Cancer Res. 75 (2015) 1423–1432.

[24] C. Jiang, F. Zuo, Y. Wang, J. Wan, Z. Yang, H. Lu, W. Chen, W. Zang, Q. Yang, J. Wang, Progesterone exerts neuroprotective effects and improves long-term neurologic outcome after intracerebral hemorrhage in middle-aged mice, Neurobiol. Aging 42 (2016) 13–24.

[25] H. Wu, T. Wu, X. Han, J. Wan, C. Jiang, W. Chen, H. Lu, Q. Yang, J. Wang, Cerebroprotection by the neuronal PGE2 receptor EP2 after intracerebral hemorrhage in middle-aged mice, J. Cerebr. Blood Flow Metab. 37 (2017) 39–51.

[26] C. Li, L. Zhu, Y. Dai, Z. Zhang, L. Huang, T.J. Wang, P. Fu, Y. Li, J. Wang, C. Jiang, Diet-induced high serum levels of trimethylamine-N-oxide enhance the cellular inflammatory response without exacerbating acute intracerebral hemorrhage injury in mice, Oxid. Med. Cell. Longev. 2022 (2022) 1599747.

[27] W. Zhu, Y. Gao, J. Wan, X. Lan, X. Han, S. Zhu, W. Zang, X. Chen, W. Ziai, D.F. Hanley, S.J. Russo, R.E. Jorge, J. Wang, Changes in motor function, cognition, and emotion-related behavior after right hemispheric intracerebral hemorrhage in various brain regions of mouse, Brain Behav. Immun. 69 (2018) 568–581.

[28] H. Yang, W. Ni, H. Jiang, Y. Lei, J. Su, Y. Gu, L. Zhou, Histone deacetylase inhibitor scriptaid alleviated neurological dysfunction after experimental intracerebral hemorrhage in mice, Behav. Neurol. 2018 (2018) 6583267.

[29] M.V. Tribulatti, J. Carabelli, C.A. Prato, O. Campetella, Galectin-8 in the onset of the immune response and inflammation, Glycobiology 30 (2020) 134–142.

[30] E. Parada, A.I. Casas, A. Palomino-Antolin, V. Gomez-Rangel, A. Rubio-Navarro, V. Farre-Alins, P. Narros-Fernandez, M. Guerrero-Hue, J.A. Moreno, J.M. Rosa, J.M. Roda, B.J. Hernandez-Garcia, J. Egea, Early toll-like receptor 4 blockade reduces ROS and inflammation triggered by microglial pro-inflammatory phenotype in rodent and human brain ischaemia models, Br. J. Pharmacol. 176 (2019) 2764–2779.

[31] S. Fujimoto, H. Katsuki, M. Ohnishi, M. Takagi, T. Kume, A. Akaike, Thrombin induces striatal neurotoxicity depending on mitogen-activated protein kinase pathways in vivo, Neuroscience 144 (2007) 694–701.

[32] J. Wang, Preclinical and clinical research on inflammation after intracerebral hemorrhage, Prog. Neurobiol. 92 (2010) 463–477.

[33] V. Cattaneo, M.V. Tribulatti, J. Carabelli, A. Carestia, M. Schattner, O. Campetella, Galectin-8 elicits pro-inflammatory activities in the endothelium, Glycobiology 24 (2014) 966–973.

[34] M.A. Romaniuk, M.V. Tribulatti, V. Cattaneo, M.J. Lapponi, F.C. Molinas, O. Campetella, M. Schattner, Human platelets express and are activated by galectin-8, Biochem. J. 432 (2010) 535–547.

[35] A. Shtaya, L.R. Bridges, M.M. Esiri, J. Lam-Wong, J.A.R. Nicoll, D. Boche, A.H. Hainsworth, Rapid neuroinflammatory changes in human acute intracerebral hemorrhage, Ann Clin Transl Neurol 6 (2019) 1465–1479.

[36] S.A. Liddelow, B.A. Barres, Reactive astrocytes: production, function, and therapeutic potential, Immunity 46 (2017) 957–967.

[37] S.A. Liddelow, K.A. Guttenplan, L.E. Clarke, F.C. Bennett, C.J. Bohlen, L. Schirmer, M.L. Bennett, A.E. Münch, W.S. Chung, T.C. Peterson, D.K. Wilton, A. Frouin, B.A. Napier, N. Panicker, M. Kumar, M.S. Buckwalter, D.H. Rowitch, V.L. Dawson, T.M. Dawson, B. Stevens, B.A. Barres, Neurotoxic reactive astrocytes are induced by activated microglia, Nature 541 (2017) 481–487.

[38] M. Shiratori, H. Tozaki-Saitoh, M. Yoshitake, M. Tsuda, K. Inoue, P2X7 receptor activation induces CXCL2 production in microglia through NFAT and PKC/MAPK pathways, J. Neurochem. 114 (2010) 810–819.

[39] N. Nishi, H. Shoji, M. Seki, A. Itoh, H. Miyanaka, K. Yuube, M. Hirashima, T. Nakamura, Galectin-8 modulates neutrophil function via interaction with integrin alphaM, Glycobiology 13 (2003) 755–763.

[40] J. Carabelli, V. Quattrocchi, A. D'Antuono, P. Zamorano, M.V. Tribulatti, O. Campetella, Galectin-8 activates dendritic cells and stimulates antigen-specific immune response elicitation, J. Leukoc. Biol. 102 (2017) 1237–1247.

[41] D. Weinmann, M. Kenn, S. Schmidt, K. Schmidt, S.M. Walzer, B. Kubista, R. Windhager, W. Schreiner, S. Toegel, H.J. Gabius, Galectin-8 induces functional disease markers in human osteoarthritis and cooperates with galectins-1 and -3, Cell. Mol. Life Sci. 75 (2018) 4187–4205.